

# Diagnosis of prostate cancer by quantitative analysis of 3DMRSI data: A new model<sup>\*</sup>

QUAN Hong<sup>1</sup>, WANG Xiaoying<sup>2</sup>, BAO Shanglian<sup>1\*\*</sup>,  
WANG Huiliang<sup>1</sup>, LI Feiyu<sup>2</sup> and HUANG Rong<sup>2</sup>

(1. The Research Center for Tumor Diagnosis and Therapeutical Physics and the Beijing Key Laboratory of Medical Physics and Engineering, Peking University, Beijing 100871, China; 2. Department of Radiology, The First Affiliated Hospital, Peking University, Beijing 100034, China)

Received July 30, 2004; revised September 10, 2004

**Abstract** Three-dimensional magnetic resonance spectroscopic imaging (3DMRSI) is helpful to identify prostate cancer (PC) from benign prostate hyperplasia (BPH) and to show the distribution of tumor infiltration. Combined with the (Cho+Cre)/Cit ratio, the z-score model can effectively discriminate prostate cancer from stromal benign prostate hyperplasia (sBPH) and detect small malignant lesions (SML).

**Keywords:** three dimensional magnetic resonance spectroscopic imaging (3DMRSI), prostate cancer, z-score model.

Prostate cancer (PC) has the highest morbidity rate in male urinary system disorders in Europe and America, and it is one of the primary reasons of male death<sup>[1]</sup>. In China, although the attack of PC is relatively low, it has a growing trend in recent 10 years<sup>[2-4]</sup>. In clinical practice, magnetic resonance imaging (MRI) could provide high resolution morphological structure and has the capability of multi-parameter imaging, but it cannot reliably differentiate PC from benign prostate hyperplasia (BPH) and normal tissues, particularly for the patients with some treatment<sup>[1,3]</sup>.

Clinically, the (choline + creatine)/citrate ratio (simplified as (Cho+Cre)/Cit) is usually significant in the diagnosis of PC<sup>[5-9]</sup>. Malignant epithelial cells have a reduced capacity of synthesis and secretion of Cit, leading to the reduction of Cit content in PC tissue compared with that in normal tissue; Cho is involved in membrane synthesis and degradation, and it is increased in PC; Cre is not significantly different between PC and BPH in magnetic resonance spectroscopic imaging, the Cre peak (located at 3.0 ppm) overlaps the Cho peak (located at 3.2 ppm). Kurhanewicz et al. reported that the mean value of (Cho+Cre)/Cit in American patients with PC was 2.10, and BPH was 0.61<sup>[1]</sup>. The mean value of (Cho+Cre)/Cit in Chinese patients with PC was re-

ported to be  $2.53 \pm 1.02$ , while it was 0.62 for BPH<sup>[4]</sup>. Three-dimensional magnetic resonance spectroscopic imaging (3DMRSI) is a noninvasive method to get information on metabolites distribution *in vivo*, and it has been shown to be an effective tool in differentiating PC from BPH when combined with MRI.

Several drawbacks exist in previous studies. First, they cannot assess the spatial distribution of observed metabolic changes. Most of these studies usually correlated one voxel's (Cho+Cre)/Cit ratio in the excitation region with systematic biopsy findings, that is, imaging in single-voxel rather than in multi-voxel. Secondly, these studies were only based on a large quantity of statistical data, without using an effective model for discrimination of individual patients. In this situation, early carcinoma and small lesion of the cancer are easy to be missed. Moreover, using (Cho+Cre)/Cit only is not reliable to identify PC from stromal BPH (sBPH) because the (Cho+Cre)/Cit ratio of sBPH is partially overlapped with PC<sup>[1,4-6]</sup>.

To solve these problems, we employed 3DMRSI to display spatial distribution of the high metabolic region, and used the z-score model combined with the ratio of (Cho+Cre)/Cit to distinguish benign from

<sup>\*</sup> Supported by National Natural Science Foundation of China (Grant Nos. 10275003 and 10175004) and the Natural Science Foundation of Beijing (Grant No. 3011002)

<sup>\*\*</sup> To whom correspondence should be addressed. E-mail: bao@pku.edu.cn

malignant tumor. The method was verified to be very effective by postoperative histological findings.

## 1 Materials and methods

### 1.1 Subjects

Fourteen subjects (at age of 57–87) with prostate disease were studied with MRI and 3DMRSI at The First Affiliated Hospital, Peking University. Among them, 9 patients were diagnosed with BPH, and 5 were PC patients, proved by transurethral US (TRUS)-guided biopsy assessed on 6 punctures in sextant or 13 punctures in quintant (region). The operation physician recorded positions of biopsy and drew maps. The puncture was perforated by a 16G needle and the tissue was semi-cylindrical with a length of 2 cm.

### 1.2 MRI and MRSI examinations

#### 1.2.1 Coil placement

The abdomen phased-array coil was tightly secured over the pelvis. The posterior and anterior coil plates were positioned with the same superior-to-inferior isocenter. A belt placed over the upper margin of the phased-array coil reduced the effect of motion. 3DMRSI was performed with abdomen phased-array coil and expandable endorectal coil. The endorectal coil was inflated with 30–100 mL of air and pulled back and secured so that it did not move within the rectal ampulla.

#### 1.2.2 MR scanning

All examinations were performed by a 1.5T GE Signa system with a body coil for radio-frequency transmission and an expandable coil as part of a pelvic phased-array arrangement to receive the MR signals, and a rectum RF coil for further signal enhancement. A fast spin-echo (FSE) sequence was used to acquire all T<sub>2</sub>WI; TR/TE= 3500/85 ms, ETL19, 5 mm slices, 0.5 mm section gap, 240 mm FOV, 4NEX, 320×256 matrix. T<sub>1</sub>WI was acquired with a conventional spin-echo sequence. Using the pelvic phased-array coil connected with an endorectal RF coil for further enhancement, T<sub>1</sub>-weighted axial images were obtained from the symphysis pubis to the aortic bifurcation, and T<sub>1</sub>-weighted sagittal images were obtained in the median pelvic cavity under the conditions of TR 450–500 ms, TE 12 ms, 5–8 mm slices, 1–2 mm section gap, 280–400 mm FOV,

2NEX, 256×192 matrix.

#### 1.2.3 3DMRSI scanning

3D MRSI was performed with the PRESS volume-selection technique and PROSE sequence of TR/TE= 1000/130 ms, the scan time was about 18 min. From the high-resolution axial T<sub>2</sub>WI, a spectroscopy volume was selected to encompass as much of the prostate as possible while excluding periprostate lipids and gas in the rectum. The position of the selected volume and the efficacy of localization were evaluated by imaging the selected volume in an axial orientation. Saturated belt (VSS pulse) was used at the edge of the ROI to suppress lipid, and to minimize the impact of gas located at the back of the prostate if necessary. Routine pre-scanning, including automatic uniform of field and suppression of water, was performed before acquiring 3DMRSI data usually when the line width was less than 15.

### 1.3 Data processing and analysis

#### 1.3.1 Model of data analysis

An automatic statistical analysis model developed by McKnight et al. was used to identify the tumor tissue of PC<sup>[10]</sup>. The model was developed based on two assumptions. First, it assumes that the variation in cell density due to partial volume effects did not significantly affect the relative ratio of (Cho+Cre) to Cit in normal tissues; second, it assumes that the variation of the ratio of (Cho+Cre)/Cit in normal tissue was small when compared with the difference between normal and diseased tissue. With these assumptions in mind, the (Cho+Cre) level could be plotted against the Cit level and fit with a linear regression. Then (residual<sup>μ</sup>) (μ is mean value) and standard deviation (SD) of the perpendicular residual distance between each point and the regression line were estimated. The criterion for normality was a z-score ( $z = (\text{residual}^\mu) / \text{SD}$ ) of less than 2, which corresponds to 95% probability of that the voxel belonged to the fitted population. Points that did not meet the criterion were excluded from the model, and a new regression line was calculated through the remaining points. This process was repeated until no points were excluded. The remaining points were the control population that was used to estimate the normal ratios of (Cho+Cre)/Cit. Once the control population of points was defined, the residual z-score of each voxel within the PRESS box was calculated and

was used to estimate the probability of malignancy with the criteria of  $z$ -score above 2.

### 1.3.2 Data processing

All raw spectral data was transferred to a workstation (SUN GE Adw 4.0) for processing, and an automatic processing software developed by our group was used to do the analysis. The process of the analysis was: (1) to define the peak position of metabolites (the peak positions of Cho, Cre and Cit were located at 3.2 ppm, 3.0 ppm and 2.65 ppm respectively); (2) to calculate the ratio of signal to noise (SNR) for all voxels in ROI and determine the effective voxels, which were defined for voxels with SNR greater than 5, for further analysis; (3) to count the  $z$ -score and the ratio of  $(\text{Cho} + \text{Cre})/\text{Cit}$  for the effective voxels; (4) to show the regions of  $z$ -score greater than 2 in ROI, which correspond to cancer occurrence. At

the same time, to display the regions of  $(\text{Cho} + \text{Cr})/\text{Cit}$  greater than 0.86 for comparison with the region of  $z$ -score greater than 2 (according to WANG et al., the cutoff value of  $(\text{Cho} + \text{Cre})/\text{Cit}$  of PC and non-PC for Chinese adult was  $0.86^{[4]}$ ).

## 2 Results

All 5 PC samples showed high metabolic activity regions in the periphery zone (PZ), and cancer was found at the overlapped area of the two high metabolic regions, and the result was confirmed by puncture biopsy. Fig. 1 illustrates the calculated result of one PC patient, in which (a) exhibits the scanning position, and the white frame corresponds to the excitation region of MRSI examination; (b) displays the corresponding spectra of (a); (c) presents the result of TRUS-guided puncture biopsy for this patient, it

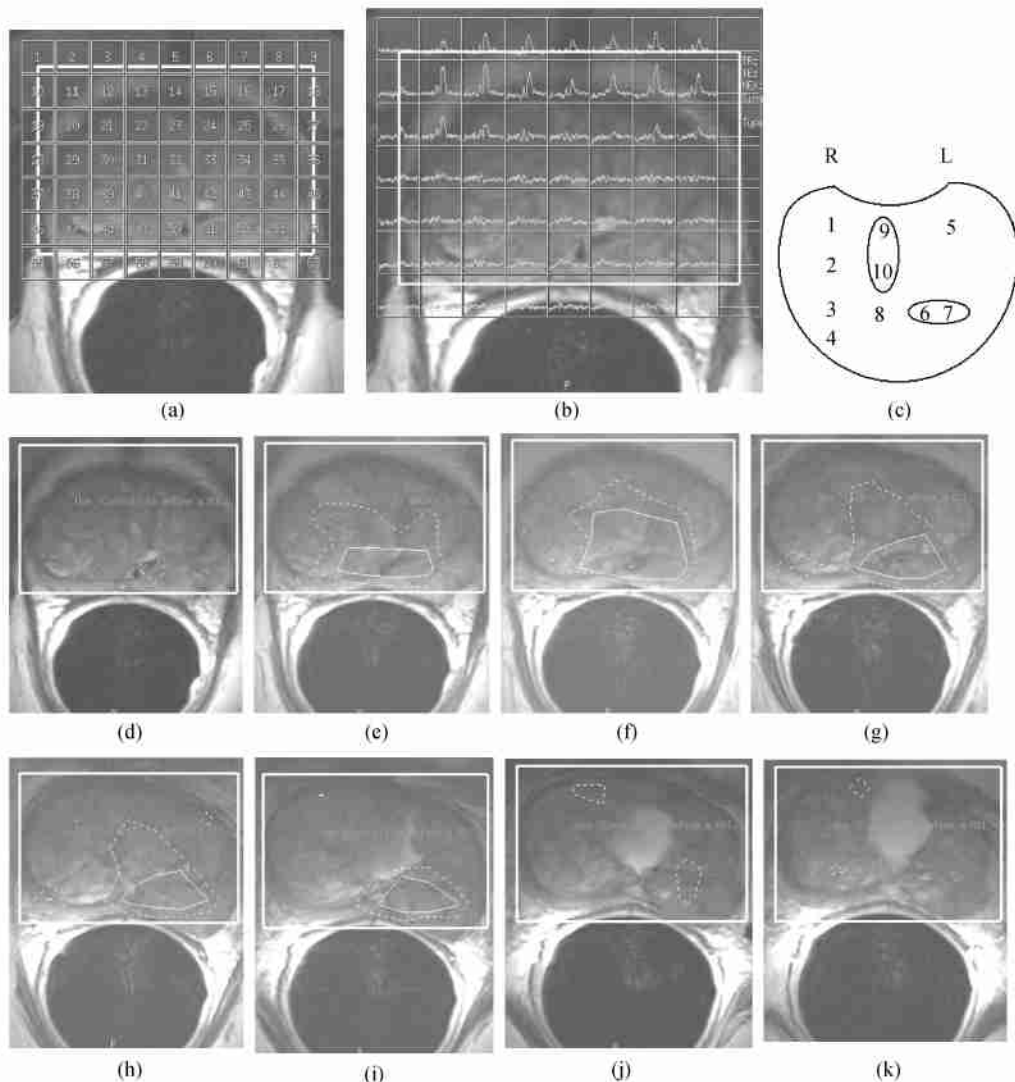


Fig. 1. Results of one PC patient. Punctures 6, 7, 9 and 10 had tumour tissue. From (a) to (k), see text.

is the frontal surface of the prostate at coronal orientation, and L represents left side while R indicates the right side. Punctures 6, 7, 9 and 10 were verified to be cancerization in (c); (d)–(k) show the excitation position located by 3DMRSI and display apparently high metabolic activity regions from the bottom to the top of the prostate. The white solid line corresponds to z-score greater than 2, while the white dotted line relates to the ratio of  $(Cho+Cre)/Cit$  greater than 0.86. The two regions were both considered to be abnormal metabolism. It is noticed that the overlapped areas of two abnormal metabolic regions appear in Fig. 1 (e) to (i) but not in (d), (j) and (k), and these overlapped areas were supposed to have tumor cells while those abnormal metabolic regions without overlapping in (d), (j) and (k) were presumed not to be malignant. The assumption was verified by the puncture biopsy findings.

Fig. 2 illustrates the results of another PC case. The excitation region and the calculated results of high metabolic area of one slice are displayed in (a), while the map of TRUS-guided puncture biopsy is presented in (b). The pathological map in (b) shows punctures 1 and 4 are tumor tissues. Fig.3 displays

the results of a small malignant lesion (SML), in which, (a) and (b) show the excitation position and the high metabolic activity region of the two continuous bottom slices of prostate; (c) is the map of the puncture biopsy exhibition, and puncture 5 is the tumor tissue. Figs.1–3 all show that tumor occurs at the overlapped area of the region of z-score greater than 2 and the region of the  $(Cho+Cr)/Cit$  ratio greater than 0.86.

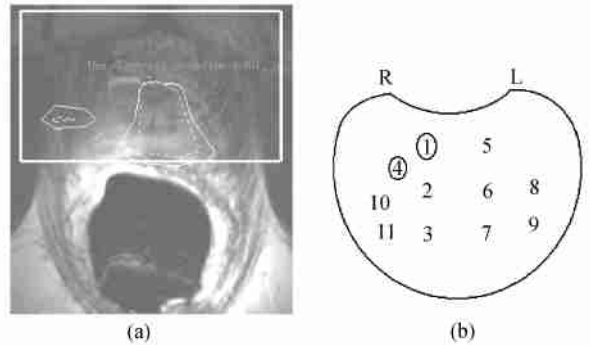


Fig. 2. One slice of a patient with PC. Punctures 1 and 4 had tumor tissues. (a) The excitation region and the calculated results of high metabolic area of one slice; (b) the map of TRUS-guided puncture biopsy.

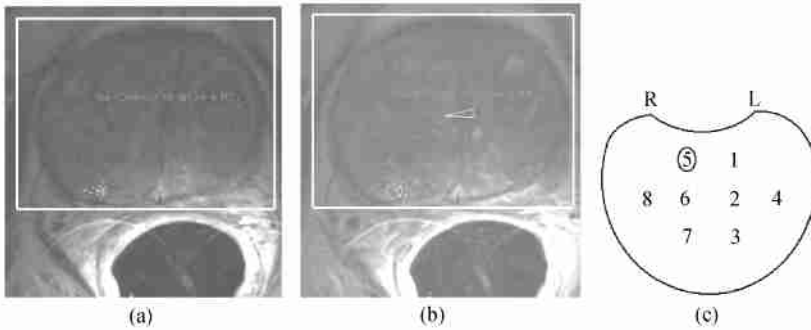


Fig. 3. Results of a patient with small lesion of PC. Puncture 5 had tumor tissue. (a) and (b), The excitation position and the high metabolic activity region of the two continuous bottom slices of prostate; (c) the map of the puncture biopsy.

Most of the regions of abnormal metabolism found in 9 BPH patients were located in the central gland (CG) or near urinary tissue while only a few were located in PZ. For those patients with an abnormal metabolism in PZ, no overlapped areas were found. Fig. 4 shows an example of BPH. Abnormal metabolism of PZ is displayed in (a) and (b), but no overlap of solid line and dotted line is found. This shows that they are benign proliferation. The presumption was verified by biopsy.

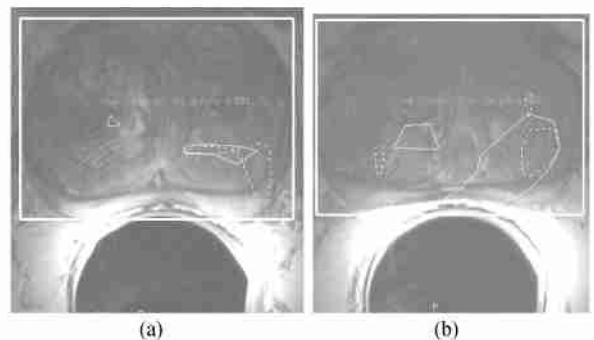


Fig. 4. Results of a patient with BPH. No overlapped area of the two high metabolic regions was seen in peripheral zone. (a) and (b), The excitation position and the high metabolic activity region of the two slices of prostate.

### 3 Discussion and conclusion

Diagnosis of PC needs to discriminate areas of PC from BPH and normal prostate tissue noninvasively as well as to estimate its range of distribution, and the stages of PC also need to be accurately determined before surgery. Conventional imaging techniques, such as MRI and transrectal ultrasound, cannot give confirmative results in distinguishing PC from BPH to some degree, especially after surgery and biopsy operations. Serum prostate specific antigen (PSA) level has been shown to be elevated in patients with PC, but it is not a specific criterion and does not provide information about the infiltration of the cancer. The commonly used method for distinguishing PC from BPH remains histological analysis of biopsy samples, which is invasive and subject to large sampling errors. 3DMRSI was reported to be helpful to solve these problems<sup>[1-8]</sup>.

Although the ratio of  $(\text{Cho} + \text{Cre})/\text{Cit}$  was informative for distinguishing PC from glandular BPH (gBPH), it is difficult to discriminate PC from stromal BPH (sBPH) and to detect SML<sup>[1,4-6]</sup>. The  $(\text{Cho} + \text{Cre})/\text{Cit}$  ratio of sBPH is similar to PC because the lowered level of Cit increases  $(\text{Cho} + \text{Cre})/\text{Cit}$  ratio of sBPH, while the  $(\text{Cho} + \text{Cre})/\text{Cit}$  ratio of SML is not high due to less prominent decreased Cit level in each voxel. In this situation, the SML would be easily missed. In contrast, the residual z-score model is calculated by using individual  $(\text{Cho} + \text{Cre})$  and Cit levels in each voxel instead of the ratio of  $(\text{Cho} + \text{Cre})/\text{Cit}$ , and the Cho level, which is a sensitive index for tumor growth, is emphasized in z-score model. The z-score of sBPH is not high due to its less prominent Cho level even if it has relatively high  $(\text{Cho} + \text{Cre})/\text{Cit}$  ratio, while the z-score of SML is elevated due to its raised Cho level even if it has a relatively low  $(\text{Cho} + \text{Cre})/\text{Cit}$  ratio. Therefore, the z-score model combined with the  $(\text{Cho} + \text{Cre})/\text{Cit}$  ratio will be more valuable in diagnosis of prostate diseases by MRSI. This method is feasible in our primary test, but its potential in the diagnosis of PC needs further verification on a large scale clinical test.

Combined with the structure imaging provided by MRI, 3DMRSI can present the infiltration extent of tumor, which is very important for designing treatment plans<sup>[6,8]</sup> for each patient. For surgery and implant radiotherapy, the appropriate treatment plan can be implemented according to the tumor volume as shown in Figs. 1-3. Definition of accurate tumor

volume may focus the radiation dose on tumor tissues and protect peripheral normal tissues especially for implant radiotherapy<sup>[8]</sup>. To determine the cutoff value of MRSI for Chinese patients with PC, however, the correlation of the  $(\text{Cho} + \text{Cre})/\text{Cit}$  ratio with the ratio determined at step-section histological examination of the excised gland should be the subject of further investigation. With the limitations of the range and the sampling errors, systematic puncture biopsy verifies easily advanced and more invasive lesions while misses those early and less invasive lesions<sup>[4]</sup>. In our experiment the overlapped area shown in Fig. 4 (b) could not be reached by puncture, so we could not determine whether the region is normal or cancerous.

In general, 3DMRSI can display the distribution of tumor cells in the whole prostate. Combined with the ratio of  $(\text{Cho} + \text{Cre})/\text{Cit}$ , the z-score model can effectively identify PC from BPH and detect SML. Nevertheless, more work still should be done to make MRSI become a routine examination method for diagnosis of PC.

### References

- 1 Kuhnawicz J., Vigneron D. B., Hricak H. et al. Three-dimensional <sup>1</sup>H spectroscopic imaging of the *in situ* human prostate with high (0.24-0.7 cm<sup>3</sup>) spatial resolution. *Radiology*, 1996, 198: 795-805.
- 2 Wang X. Y., Zhou L. P. and Jiang X. X. Three-dimensional <sup>1</sup>H MR spectroscopic imaging of the prostate: Preliminary results. *China JMIT*, 2002, 18: 1154-1157.
- 3 Wang X. Y., Jiang X. X., Xiao J. X. et al. Evaluation therapeutic effectiveness of endocrine treatment for patients with prostate cancer by MRI. *China J. Radiol.*, 2000, 34: 402-404.
- 4 Wang X. Y., Zhou L. P., Ding J. P. et al. Quantitative analysis of prostate adenocarcinoma by MRS: Correlation study with systematic biopsy. *China J. Radiol.*, 2004, 38: 368-372.
- 5 Garcia-Segura J. M., Sanchez-Chapado M., Ibarburen C. et al. *In vivo* proton magnetic resonance spectroscopy of diseased prostate: Spectroscopic features of malignant versus benign pathology. *Magn. Reson. Imaging*, 1999, 17(5): 755-765.
- 6 Kuhnawicz J., Vigneron D. B., Hricak H. et al. Prostate cancer: metabolic response to cryosurgery as detected with 3D <sup>1</sup>H MR spectroscopic imaging. *Radiology*, 1996, 200: 489-496.
- 7 Scheidler J., Hricak H., Vigneron D. B. et al. Prostate cancer: localization with three-dimensional proton MR spectroscopic imaging-clinicopathology study. *Radiology*, 1999, 213: 252-358.
- 8 Zaider M., Zelefsky M. J., LEE E. et al. Treatment planning for prostate implants using magnetic resonance spectroscopy imaging. *Int. J. Radiation Oncology Biol. Phys.*, 2000, 47(4): 1085-1096.
- 9 Menard C., Smith C. P., Somorjai R. L. et al. Magnetic resonance spectroscopy of the malignant prostate gland after radiotherapy: A histopathologic study of diagnostic validity. *Int. J. Radiation Oncology Biol. Phys.*, 2001, 50(2): 317-323.
- 10 Mcknight T. R., Noworolski S. M., Vigneron D. B. et al. An automated technique for the quantitative assessment of 3D-MRSI data from patients with glioma. *JMRI*, 2001, 13: 167-177.